PNAS PLUS

Control of MT1-MMP transport by atypical PKC during breast-cancer progression

Carine Rossé[a,b,1], Catalina Lodillinsky[a,b], Laetitia Fuhrmann[a], Maya Nourieh[a], Pedro Monteiro[a,b,c], Marie Irondelle[a,b], Emilie Lagoutte[a,b], Sophie Vacher[d], François Waharte[a,e], Perrine Paul-Gilloteaux[a,e], Maryse Romao[a,f], Lucie Sengmanivong[a,e,g], Mark Linch[h], Johan van Lint[i], Graça Raposo[a,f], Anne Vincent-Salomon[a,j,k], Ivan Bièche[d], Peter J. Parker[h,l], and Philippe Chavrier[a,b,1]

[a]Research Center, Institut Curie, 75005 Paris, France; [b]Membrane and Cytoskeleton Dynamics, Centre National de la Recherche Scientifique, Unité Mixte de Recherche 144, 75005 Paris, France; [c]Sorbonne Universités, Université Pierre et Marie Curie, University of Paris VI, Institut de Formation Doctorale, 75252 Paris Cedex 5, France; [d]Department of Genetics, Institut Curie, 75005 Paris, France; [e]Cell and Tissue Imaging Facility, Centre National de la Recherche Scientifique, Unité Mixte de Recherche 144, 75005 Paris, France; [f]Structure and Membrane Compartments, Centre National de la Recherche Scientifique, Unité Mixte de Recherche 144, 75005 Paris, France; [g]Nikon Imaging Centre, Institut Curie, Centre National de la Recherche Scientifique, 75005 Paris, France; [h]Protein Phosphorylation Laboratory, Cancer Research UK London Research Institute, London WC2A 3LY, United Kingdom; [i]Department of Molecular Cell Biology, Faculty of Medicine, Katholieke Universiteit Leuven, 3000 Leuven, Belgium; [j]Department of Tumor Biology, Institut Curie, 75005 Paris, France; [k]Institut National de la Santé et de la Recherche Médicale U830, 75005 Paris, France; and [l]Division of Cancer Studies, King's College London, Guy's Campus, London WC2A 3LY, United Kingdom

Edited by Mina J. Bissell, E. O. Lawrence Berkeley National Laboratory, Berkeley, CA, and approved March 27, 2014 (received for review January 14, 2014)

Dissemination of carcinoma cells requires the pericellular degradation of the extracellular matrix, which is mediated by membrane type 1-matrix metalloproteinase (MT1-MMP). In this article, we report a co–up-regulation and colocalization of MT1-MMP and atypical protein kinase C iota (aPKCι) in hormone receptor-negative breast tumors in association with a higher risk of metastasis. Silencing of aPKC in invasive breast-tumor cell lines impaired the delivery of MT1-MMP from late endocytic storage compartments to the surface and inhibited matrix degradation and invasion. We provide evidence that aPKCι, in association with MT1-MMP–containing endosomes, phosphorylates cortactin, which is present in F-actin–rich puncta on MT1-MMP–positive endosomes and regulates cortactin association with the membrane scission protein dynamin-2. Thus, cell line-based observations and clinical data reveal the concerted activity of aPKC, cortactin, and dynamin-2, which control the trafficking of MT1-MMP from late endosome to the plasma membrane and play an important role in the invasive potential of breast-cancer cells.

membrane traffic | actin cytoskeleton | multi-vesicular body | MMP14

Metastasis—the process by which cells from a primary tumor invade local tissues and disseminate to distant sites—marks the transition from a benign tumor to a lethal, malignant cancer. One intrinsic property of metastatic tumor cells that allows them to breach tissue barriers is their ability to degrade the proteins of the extracellular matrix (ECM). This remodeling of the ECM by cancer cells depends on matrix-degrading proteases, including matrix metalloproteinases (MMPs) (1, 2). Although secreted MMPs have been implicated in cancer for several decades, it is more recently that a subgroup of membrane-anchored MMPs, including membrane type 1 (MT1)-MMP, have been recognized as important proteases involved in dissemination of tumor cells and cancer progression (3–7).

Membrane type 1-matrix metalloproteinase (MT1-MMP) is up-regulated in human cancers, including breast cancers, and it is enriched at the front of invasive lesions (8, 9). In tumor-derived cells cultured on a flat ECM substratum, such as gelatin or type I collagen, MT1-MMP accumulates in specialized matrix-degrading plasma-membrane domains called invadopodia (10). The current view is that interaction of matrix receptors on the tumor-cell surface with components of the ECM leads to assembly of nascent invadopodia containing F-actin and cortactin, which mature into matrix-degrading invadopodia when they accumulate MT1-MMP (11).

Little is known about how invadopodia form in metastatic cells and how they are endowed with proteolytic activity. In MDA-MB-231 human breast adenocarcinoma cells, newly synthesized MT1-MMP passes through the secretory pathway to reach the plasma membrane where it is then endocytosed (12). The majority of internalized MT1-MMP is located in a late endocytic compartment from where a fraction recycles to plasma-membrane invadopodia (13). Various studies, including our own, have identified several components of the exocytic machinery that are required for delivery of MT1-MMP to invadopodia, including cortactin (a regulator of actin dynamics), the exocyst complex (required for docking of transport vesicles), and vesicle-associated membrane protein 7 (VAMP7) (a late endosome v-SNARE protein involved in vesicle fusion) (10, 13–16). Although these findings provide important insights into how MT1-MMP is delivered to the invadopodial plasma membrane, the mechanisms underlying the formation of MT1-MMP transport intermediates from late endocytic compartments remain largely unexplored.

Atypical protein kinase C (aPKC) comprises a branch of the serine/threonine PKC superfamily consisting of two isoforms, aPKCζ and aPKCι, that are distinct from the typical, diacylglycerol-regulated isoforms (17). aPKCζ/ι are activated mainly by components of the PAR complex, Cdc42 and Par-3, and play a critical role in the formation of epithelial cell–cell junctions and the development of apico-basal polarity in mammalian epithelial cells (18). Previously, we reported the role of an aPKCζ/ι–exocyst complex in signaling at the leading edge of

Significance

We characterize a mechanism through which the polarity protein atypical PKCι controls invasion and matrix remodeling by tumor cells by regulating endosome-to-plasma membrane traffic of the membrane type 1-matrix metalloproteinase (MT1-MMP) in breast-cancer cells. Further analysis shows that atypical PKCι and MT1-MMP are co–up-regulated in hormone receptor-negative breast tumors in association with higher risk of metastasis. These findings provide previously unidentified avenues for the design of therapeutic interventions.

Author contributions: C.R. and P.C. designed research; C.R., L.F., P.M., M.I., S.V., M.R., and L.S. performed research; E.L., P.P.-G., M.L., and J.v.L. contributed new reagents/analytic tools; C.R., C.L., M.N., P.M., M.I., S.V., F.W., P.P.-G., G.R., A.V.-S., I.B., P.J.P., and P.C. analyzed data; and C.R. and P.C. wrote the paper.

The authors declare no conflict of interest.

This article is a PNAS Direct Submission.

[1]To whom correspondence may be addressed. E-mail: philippe.chavrier@curie.fr or carine.rosse@curie.fr.

This article contains supporting information online at www.pnas.org/lookup/suppl/doi:10.1073/pnas.1400749111/-/DCSupplemental.

migrating cells, so controlling paxillin phosphorylation and regulating focal adhesion dynamics (19). In addition, several lines of evidence implicate aPKCζ/ι in cancer: aPKCς is required for epidermal growth factor-induced chemotaxis of human breast-cancer cells (20), and aPKCζ/ι promotes matrix degradation by Src-transformed mouse NIH 3T3 fibroblasts (21). Moreover, aPKCι expression is up-regulated in various cancers, including breast cancer, and correlates with poor prognosis (22, 23). The ability of aPKCζ/ι to control both cell polarity and the migration of cells makes it a prime candidate for a role in tumor progression and metastasis although the specific functions of aPKCζ/ι in metastatic cells are currently only poorly understood.

Here, we report an up-regulation and relocalization of MT1-MMP and aPKCι in breast-tumor samples associated with a high risk of metastasis. We found that silencing of aPKCζ/ι in human breast adenocarcinoma cell lines impairs ECM degradation and invasion of the cells into different reconstituted 3D matrix environments. These functional effects of aPKCζ/ι silencing correlate with defects in cortactin phosphorylation and distribution and dynamin-2 (dyn-2) recruitment and function on MT1-MMP–containing endosomes, resulting in impaired delivery of MT1-MMP to the invadopodial plasma membrane. This study thus identifies a previous unidentified coordinated function for aPKCζ/ι, cortactin, and dyn-2 in the control of MT1-MMP trafficking from late endosomes to the plasma membrane during breast-tumor cell invasion, providing a rationale for the design of therapeutic interventions.

Results

Co–Up-Regulation of MT1-MMP and aPKCι mRNAs Is Associated with Adverse Clinical Outcomes in Breast Cancer. In previous studies, we implicated the exocyst complex in MT1-MMP trafficking to invadopodia in MDA-MB-231 breast-tumor cells (15) and identified a coordinated function of the exocyst complex and aPKCζ/ι in migrating cells (19). MT1-MMP and aPKCι are overexpressed in various cancers, including breast cancers, and up-regulation is associated with poor prognosis (8, 9, 22, 24). These data suggested the possible interplay between MT1-MMP and aPKCζ/ι in the invasive program of breast-tumor cells. Expression of MT1-MMP and 11 aPKCζ/ι family members was investigated by qRT-PCR analysis in breast-tumor samples from 458 patients with unilateral invasive breast tumors and known long-term outcome (Table S1). MT1-MMP expression correlated most with aPKCι mRNA ($r = +0.556$, $P < 10^{-7}$) (Table 1). We looked for correlations between aPKCι and MT1-MMP mRNA status and standard clinicopathological and biological factors in this cohort. About one third of breast tumors tested (153/458) showed aPKCι mRNA overexpression (a greater than threefold increase compared with normal tissues), and 23.3% (107/458) showed MT1-MMP mRNA overexpression (Table S1). In the tumor group that overexpressed both aPKCι and MT1-MMP, we saw a statistically significant association with histopathological grade III ($P = 0.0041$), estrogen receptor (ER)-negative ($P = 0.0014$), and progesterone receptor (PR)-negative ($P = 0.001$) status, as well as with the molecular subtype ($P = 0.003$) (Table S1). Of note, 24.6% (17/69) of triple-negative breast cancers (ER^- PR^- $HER2^-$), a type of aggressive and highly proliferative tumors, overexpressed MT1-MMP and aPKCι vs. 12.8% (50/389) for the other subtypes ($P = 0.011$). Furthermore, by combining aPKCι and MT1-MMP mRNA expression status, we identified four distinct prognostic groups with significantly different metastasis-free survival (MFS) curves ($P = 0.008$) (Fig. 1*A*). The patients with the poorest prognosis had both aPKCι and MT1-MMP mRNA overexpression whereas those with the best prognosis had normal aPKCι and MT1-MMP mRNA levels.

Table 1. Correlation using the Spearman's rank correlation test between 11 genes of the PKC family and MT1-MMP mRNA expression in human breast cancer

Gene (protein)	Spearman correlation coefficient	*P**
PRKCA (PKCα)	0.233	**0.0000021**
PRKCE (PKCε)	0.045	0.34 (NS)
PRKCH (PKCη)	0.157	**0.0009**
PKN2 (PKN2)	0.061	0.19 (NS)
PRKCZ (PKCζ)	0.10	0.82 (NS)
PRKCD (PKCδ)	0.016	0.74 (NS)
PRKCQ (PKCθ)	−0.054	0.24 (NS)
PRKCI (PKCι)	0.556	**< 0.0000001**
PRKCB (PKCβ)	0.389	**< 0.0000001**
PKN1 (PKN1)	0.199	**0.000038**

Expression of genes encoding PKCs and MT1-MMP was analyzed by reverse transcriptase-quantitative polymerase chain reaction (RT-qPCR) of 458 mRNA tumor samples. Very low levels of mRNA encoding PKCγ were detectable but not reliably quantifiable by RT-qPCR assays using the fluorescence SYBR green methodology (cycle threshold > 35). NS, not significant.
**P* value of Spearman rank correlation test. In bold type, significant *P* values.

MT1-MMP and aPKCι Colocalize in Cytoplasmic Granules and at Cell–Cell Contacts in Hormone Receptor-Negative Breast-Carcinoma Cells. To investigate changes in protein levels and localization of MT1-MMP and aPKCι during breast-tumor progression, a human tissue microarray (TMA) of 68 breast tumors representative of the four main molecular subtypes (*Experimental Procedures*) was analyzed by immunohistocytochemistry (IHC), on consecutive sections (25) (Dataset S1 and Fig. 1 *B* and *C*). Compared with epithelial cells in surrounding nonneoplastic tissues, aPKCι was overexpressed in cancer cells in all subtypes whereas expression of MT1-MMP was significantly up-regulated in hormone receptor-negative tumors (ER^- PR^- $HER2^+$ and ER^- PR^- $HER2^-$) (Dataset S1, Fig. S1 *A* and *B*, and Fig. 1*D*). These data demonstrate a positive correlation between aPKCι and MT1-MMP expression in hormone receptor-negative subtypes of breast carcinomas at both the mRNA and protein levels.

aPKCι staining was restricted to the apical surface of normal breast epithelial cells lining the lumen of the duct whereas, in tumor cells, overexpressed aPKCι lost its apical localization (Fig. 1*B* and Fig. S1*C*) and showed a predominant unpolarized distribution at cell–cell contacts and cytoplasmic granules in the majority of the tumors (Fig. 1*B* and Fig. S1 *D* and *E*). There was little or no aPKCι staining in the stroma. MT1-MMP was laterally localized in luminal epithelial cells in normal tissues and also expressed in myoepithelial cells (Fig. 1*C* and Fig. S1*C*). MT1-MMP distribution was predominantly unpolarized in cancer cells in overexpressing tumors (Fig. 1*C* and Fig. S1*C*), with both a strong cell–cell contact association and a granular cytoplasmic distribution (Fig. 1*C* and Fig. S1 *D* and *E*). Thus, in contrast to their distinct localization at separate plasma-membrane domains of normal luminal breast epithelial cells, aPKCι and MT1-MMP significantly codistributed at cell–cell contacts and cytoplasmic granules, including in hormone receptor-negative tumors. These findings correlating up-regulation of aPKCι and MT1-MMP during breast-tumor progression indicate a poor prognosis for these combined markers.

aPKCζ/ι Is Required for MT1-MMP–Dependent Matrix Degradation and Breast-Tumor Cell Invasion. The functional interplay between MT1-MMP and aPKCι in tumor-cell invasion was investigated in MDA-MB-231 and BT-549 cells, two cell lines that can be classified as triple-negative breast cancer (26). Silencing of MT1-MMP expression strongly diminished invadopodial degradation of gelatin (Fig. 2 *A* and *B*) (10, 15). We investigated whether

aPKCζ/ι played a role in MT1-MMP–dependent matrix proteolysis by silencing both aPKCζ and aPKCι in these cell lines using two independent pairs of siRNAs (Fig. 2 *A* and *B*, *Insets*, immunoblots and Fig. S2 *A* and *B*) and then quantifying matrix degradation. Compared with cells treated with an irrelevant siRNA (luciferase, siLuc), these cells showed a 60–70% reduction of their degradative capacity (Fig. 2 *A* and *B* and Fig. S2 *C* and *D*). This inhibition of matrix degradation in the absence of aPKCζ/ι was not due to alteration of MT1-MMP levels in the cells (Fig. 2 *A* and *B*, *Insets*, immunoblots and Fig. S2 *A* and *B*). Furthermore, overexpression of MT1-MMP overcompensated the adverse effect of aPKCζ/ι silencing on gelatin degradation (Fig. 2*C*, compare red bars and black bars). These data indicate that aPKCζ/ι is required for matrix proteolysis by breast-tumor cells through the control of MT1-MMP function.

We further assessed the effect of aPKCζ/ι silencing on MDA-MB-231 cell invasion across a thick layer of Matrigel and on invasive migration through fibrous type I collagen because MT1-MMP is required for invasion in these environments (13, 27). Double silencing of aPKCζ and aPKCι impaired invasion in Matrigel to a similar extent to silencing of MT1-MMP itself (Fig. 2*D*). Similarly, silencing of both aPKCζ and -ι inhibited the dissemination of MDA-MB-231 cells from multicellular spheroids into the surrounding 3D gel of type I collagen (Fig. 2 *E* and

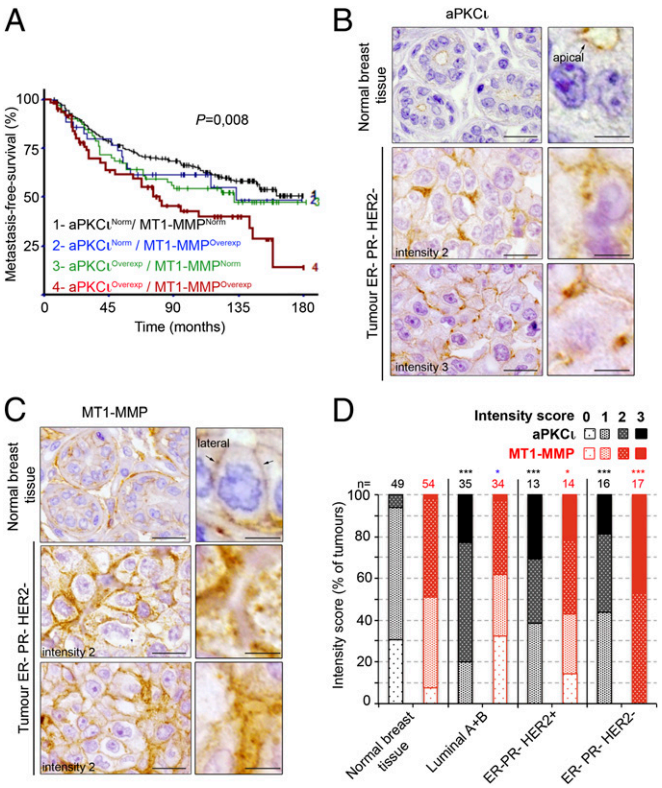

Fig. 1. Co–up-regulation and colocalization of MT1-MMP and aPKCι in hormone receptor-negative breast tumors correlate with poor prognosis. (*A*) Metastasis-free survival (MFS) curves for breast-tumor patients with normal (Norm) or overexpressed (Overexp, >3) aPKCι and MT1-MMP mRNA levels (Spearman rank). (*B* and *C*) aPKCι (*B*) and MT1-MMP (*C*) immunohistochemistry staining on consecutive sections of human breast tumor TMAs showing adjacent nonneoplastic tissue and representative ER^- PR^- $HER2^-$/triple-negative tumors. Note that adjacent nonneoplastic tissue shown in *Top* panels correspond to tumor sample shown in *Middle* panels. *Right* panels show higher magnification. [Scale bars: 20 μm (*Left*) and 5 μm (*Right*).] (D) Intensity scoring of aPKCι (black bars) and MT1-MMP (red bars) immunohistochemistry staining (on a 0-to-3 scale as documented in Fig. S1 *A* and *B*) of a tissue microarray of human breast tumors representative of the different molecular subtypes and adjacent nonneoplastic areas (Normal breast tissue). Breast molecular subtypes were defined as follows: luminal A+B according to ref. 52 [luminal A, estrogen receptor (ER) ≥ 10%, progesterone receptor (PR) ≥ 20%, Ki67 < 14%; luminal B, ER ≥ 10%, PR < 20%, Ki67 ≥ 14%]; ER– PR– HER2+, ER < 10%, PR < 10%, HER2 2+ amplified or 3+ according to ref. 53; ER– PR– HER2– (triple-negative), ER < 10%, PR < 10%, HER2 0/1+ or 2+ nonamplified according to ASCO guidelines (53). n, the number of tumors analyzed. $*P < 0.05$; $***P < 0.001$; ns, non significant compared with normal adjacent tissues (χ^2 test). Note that intensity scores of MT1-MMP expression in luminal A+B tumors are inferior to normal tissues.

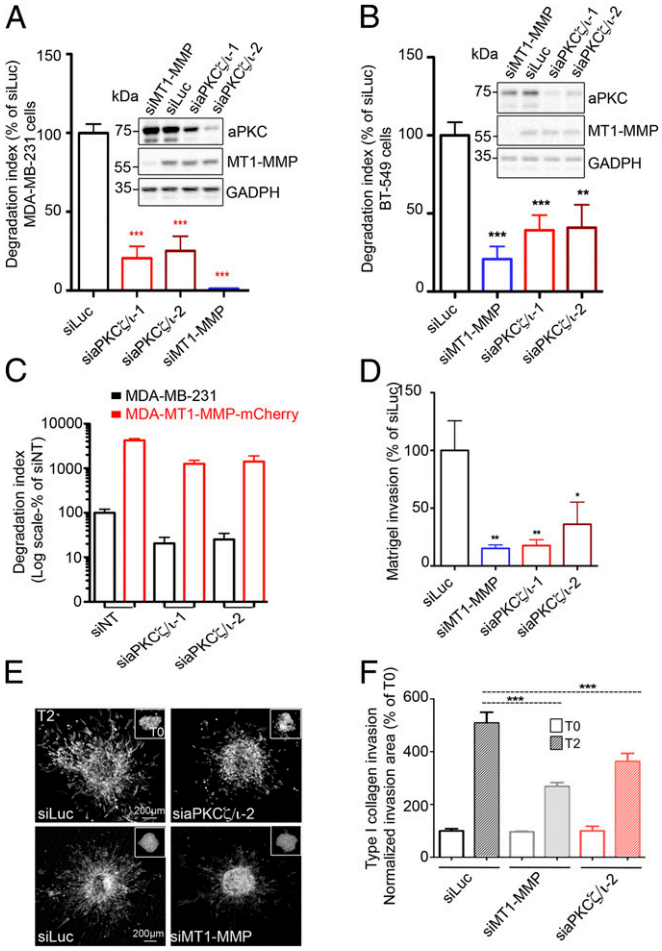

Fig. 2. Atypical PKCζ/ι regulate MT1-MMP–dependent matrix degradation and invasion. (*A* and *B*) Quantification of FITC–gelatin degradation by MDA-MB-231 (*A*) and BT-549 cells (*B*) treated with indicated siRNAs. Values are means ± SEM of the normalized degradation area from at least three independent experiments. (*Insets*) Immunoblotting with antibodies against aPKCζ/ι and MT1-MMP of cells treated with the indicated siRNAs. Immunoblotting with antibodies against GAPDH served as a control for loading. (*C*) Quantification of FITC–gelatin degradation by MDA-MB-231 stably expressing MT1-MMP–mCherry treated with the indicated siRNAs (red bars) compared with untransfected MDA-MB-231 cells (black bars). Note the logarithmic scale. (*D*) MDA-MB-231 cells treated with indicated siRNAs were tested for their ability to invade through Matrigel. Values are means ± SEM normalized to the mean for siLuc-treated cells. $*P < 0.05$; $**P < 0.01$. (*E*) Multicellular spheroids of MDA-MB-231 cells treated with siRNAs against luciferase or aPKCζ/ι (siaPKCζ/ι-2) were embedded in 3D acid-extracted type I collagen (T0) and further incubated for 2 d (T2). Images show phalloidin-labeled spheroids collected at T2 (*Insets* correspond to spheroids at T0). (Scale bars: 200 μm.) (*F*) Data are mean invasion area in type I collagen at T2 normalized to the mean invasion area at T0 ± SEM ($n = 3$ independent experiments; 15–20 spheroids were analyzed for each cell population). $***P < 0.001$.

F). These data indicate that aPKCζ/ι is required for MT1-MMP–dependent invasion of MDA-MB-231 cells in two different reconstituted matrices that mimic the 3D environment of cancer cells in vivo.

Atypical PKCζ/ι Control MT1-MMP–Containing Endosome Distribution and MT1-MMP Exocytosis. Immunoelectron microscopy of MDA-MB-231 cells stably expressing MT1-MMP–mCherry revealed association of MT1-MMP with the limiting membrane and internal luminal vesicles of vesicular compartments, with morphology typical of multivesicular bodies (Fig. 3*A*). These observations are consistent with the predominant association of MT1-MMP with VAMP7- and Rab7-positive late endocytic compartments in MDA-MB-231 cells (13, 16). Imaging of live cells expressing GFP–aPKCι revealed an association of this protein with ∼32% of MT1-MMP–mCherry–positive vesicles (Fig. 3*B* and Fig. S2*E*), reminiscent of the colocalization of aPKCι and MT1-MMP on cytoplasmic granular compartments in hormone receptor-negative breast carcinoma (Fig. 1*C* and Fig. S1*E*).

We investigated whether aPKCζ/ι may be required for MT1-MMP trafficking to the plasma membrane. Expression of a constitutively active allele of aPKCι resulted in an ∼1.5-fold increase of the density of MT1-MMP–containing vesicles in the vicinity of the plasma membrane visualized by total interference reflection fluorescence microscopy (TIRFM) (Fig. 3 *C* and *D* and Fig. S2*F*). On the contrary, aPKCζ/ι depletion induced a twofold reduction in MT1-MMP–positive endosomes at the plasma membrane (Fig. 3*E* and Fig. S2*G*). The contribution of aPKCζ/ι to MT1-MMP delivery to the invadopodial plasma membrane was assessed by quantifying surface accumulation of MT1-MMP–pHluorin (28); fluorescence of this construct is eclipsed in the acidic environment of the late endosome and rises immediately upon exocytosis and exposure to the extracellular pH (29). As expected, MT1-MMP–pHluorin accumulated at the level of cortactin-positive invadopodia on the ventral cell surface (Fig. 3*F*). Knockdown of aPKCζ/ι led to a 40–60% reduction of plasma-membrane accumulation of MT1-MMP–pHluorin, similar to the effect of cortactin siRNA, which is required for MT1-MMP delivery to invadopodia (10, 14) (Fig. 3*G*). All together, these data reveal that aPKCζ/ι controls the polarization of MT1-MMP–positive endosomes to the cell surface and MT1-MMP exocytosis and regulates pericellular matrix remodeling.

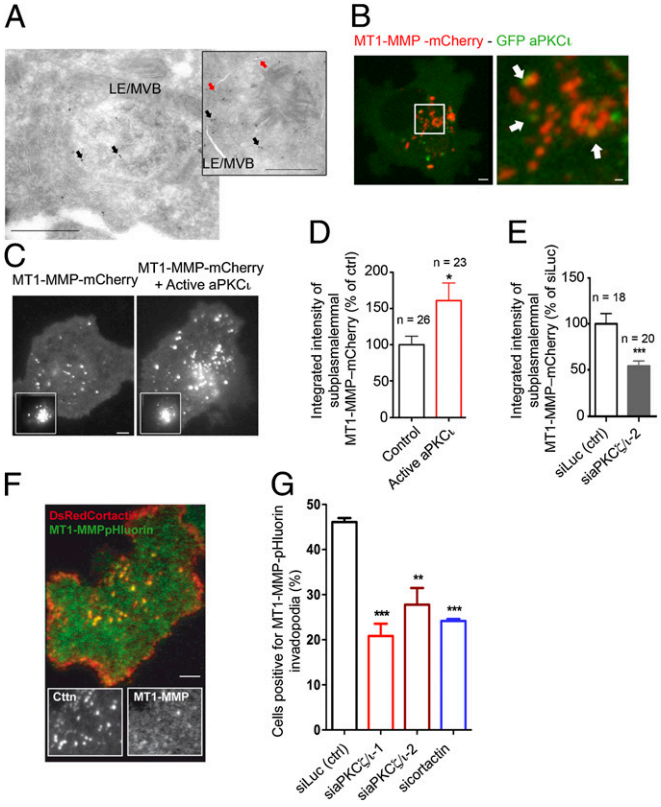

Fig. 3. aPKCζ/ι regulate MT1-MMP trafficking to plasma membrane invadopodia. (*A*) Ultrathin cryosection of MDA-MB-231 cells expressing MT1-MMP–mCherry labeled with MT1-MMP antibody followed by protein A-gold. Red arrows, MT1-MMP in the limiting membrane; black arrows, MT1-MMP associated with intraluminal vesicles of late endosomes/multivesicular bodies (LE/MVB). (Scale bars: 500 nm.) (*B*) Confocal spinning-disk microscopy image of an MDA-MB-231 cell expressing GFP–aPKCι and MT1-MMP–mCherry. [Scale bars: 5 μm (*Left*) and 1 μm (*Right*, boxed region at higher magnification). (*C*) MDA-MB-231 expressing MT1-MMP–mCherry alone or together with constitutively active aPKCι were imaged by TIRFM. (*Insets*) Corresponding wide-field images showing equal MT1-MMP expression. (Scale bar: 5 μm.) (*D* and *E*) Integrated intensity of MT1-MMP–mCherry signal per unit membrane area measured from TIRFM images. Values represent mean percentage of membrane MT1-MMP normalized to cells expressing only MT1-MMP–mCherry (*D*) or siLuc-treated cells (*E*) ± SEM. $*P < 0.05$; $***P < 0.001$. (*F*) MDA-MB-231 cells expressing MT1-MMP–pHluorin and DsRed-cortactin plated on cross-linked gelatin and analyzed by dual color TIRFM. (*Insets*) Split signals from the boxed region. (Scale bar: 5 μm.) (*G*) Plots show the percentage of cells with MT1-MMP–pHluorin–positive invadopodia. Efficiency of cortactin knockdown is shown in Fig. 4*G*. Values are means ± SEM from three independent experiments scoring a total of 150–200 cells for each cell population. $**P < 0.01$; $***P < 0.001$ (compared with cells treated with siLuc siRNA).

Dynamin-2 Associates with Cortactin on MT1-MMP–Positive Endosomes in an aPKCζ/ι-Dependent Manner and Is Required for MT1-MMP Trafficking and Matrix Degradation. Analysis of the subcellular distribution of cortactin by indirect immunofluorescence in MDA-MB-231 cells revealed that, in addition to its invadopodial location (Fig. 3*F* and Fig. S2 *C* and *D*) (10, 14), cortactin also accumulated in the central region of the cell and was dynamically associated with MT1-MMP–containing endosomes (more than 95% of MT1-MMP–positive endosomes harbored at least one cortactin-rich puncta) (Fig. 4*A* and Movie S1). In addition, F-actin and the p34-Arc subunit of Arp2/3 complex, which are components of the cytoskeleton and partner proteins of cortactin, colocalized with cortactin patches on MT1-MMP–containing endosomes in MDA-MB-231 and BT-549 cells (Fig. S3 *A*–*C*). High-resolution structured illumination microscopy revealed the presence of distinct submicrometer-sized cortactin domains associated with MT1-MMP–positive endosomes (Fig. S3*D*). Knockdown of aPKCζ/ι induced coalescence of the cortactin domains on MT1-MMP–containing endosomes (Fig. 4*A* and Fig. S3*D*) and a dramatic ∼80% increase of cortactin on MT1-MMP–positive endosomes (Fig. 4*B*). These data demonstrate that cortactin associates with F-actin assemblies on MT1-MMP–positive endosomes in an aPKCζ/ι-regulated manner.

The endosomal actin and cortactin cytoskeleton is known to regulate the formation and fission of tubulovesicular transport carriers involved in the recycling of surface proteins within the endocytic pathway (30, 31). We looked at the dynamic distribution of the late endocytic marker GFP–Rab7, which is associated with MT1-MMP–positive endosomes and colocalizes with endosomal cortactin (Fig. S3*E*) (32). By live-cell imaging, we observed the formation of GFP–Rab7-positive tubules emanating from MT1-MMP–containing endosomes and the fission of these tubules (Fig. S3*F*, *Upper*). Silencing of aPKCζ/ι, by contrast, was accompanied by more persistent Rab7– and MT1-MMP–containing tubular extensions (Fig. S3 *E*, *Right* and *F*, *Lower*), suggesting that aPKCζ/ι controls MT1-MMP–containing late endosome membrane remodeling.

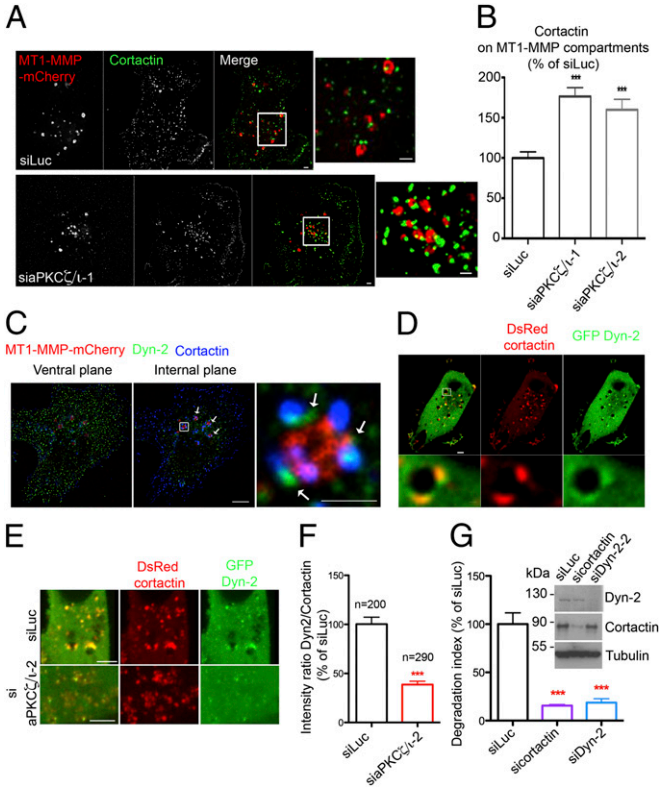

Fig. 4. aPKCζ/ι regulates cortactin and dynamin-2 recruitment on MT1-MMP–positive endosomes. (*A*) MDA-MB-231 cells stably expressing MT1-MMP–mCherry (red) were treated with indicated siRNAs, plated on gelatin, and immunolabeled with an antibody against cortactin (in green). [Scale bars: 5 μm (entire cell) and 1 μm (boxed region at higher magnification, *Right* panel of each row).] (*B*) Quantification of cortactin on MT1-MMP–mCherry–containing vesicles in deconvoluted image stacks of MDA-MD-231 cells as in *A*. The *x* axis indicates mean cortactin intensity associated with MT1-MMP–mCherry–containing endosomes normalized to the value in control siLuc-treated cells (in percentage) ± SEM (from 50 cells from each cell population). ***$P < 0.001$. (*C*) MDA-MB-231 cells expressing MT1-MMP–mCherry (red) were immunolabeled for cortactin (blue) and dyn-2 (green). (*Left*) The distribution of dyn-2 on the ventral plane of the cell in clathrin-coated pits with partial association with cortactin. (*Center*) Documents dyn-2's association with cortactin-positive puncta on MT1-MMP–mCherry vesicles (arrows). (*Right*) A higher magnification of the boxed region. [Scale bars: 5 μm (*Left* and *Center*) and 1 μm (*Right*)]. (*D*) Confocal spinning-disk microscopy image of MDA-MB-231 cells expressing GFP–dyn2 and DsRed–cortactin (Movie S2). [Scale bars: 5 μm (*Upper*) and 1 μm (*Lower*). (*E*) Dual-color confocal spinning-disk microscopy of MDA-MB-231 cells expressing DsRed–cortactin and GFP–dyn-2 and treated with indicated siRNAs. (Scale bars: 5 μm.) (*F*) The ratio of signal intensities from GFP–dyn-2 and DsRed–cortactin was measured for 200 and 290 endosomal cortactin patches in cells treated with siRNAs against luciferase or aPKC, respectively. ***$P < 0.001$. (*G*) Quantification of gelatin degradation by MDA-MB-231 cells treated with indicated siRNAs. Values are means ± SEM of the normalized degradation area from three independent experiments. (*Inset*) Immunoblotting with indicated antibodies using tubulin as a control for loading.

Cortactin regulates membrane dynamics through its interaction with dyn-2, which is involved in membrane scission and is required for the formation and function of invadopodia (33, 34). We therefore analyzed the location of endogenous dyn-2 and cortactin by immunolabeling MDA-MB-231 cells stably expressing MT1-MMP–mCherry. This immunolabeling revealed a close apposition of dyn-2 patches with cortactin puncta on ∼90% of MT1-MMP–positive endosomes (Fig. 4*C*, internal plane). Note that, as expected, dyn-2 associated with clathrin-coated pits on the plasma membrane with partial colocalization with cortactin (Fig. 4*C*, ventral plane). When coexpressed with DsRed–cortactin, GFP–dyn-2 colocalized with cortactin domains on vesicular structures in the central-cell region (Fig. 4*D* and Movie S2). In addition, deletion of the proline-rich domain (ΔPRD) of dyn-2, which mediates its interaction with the SH3 domain of cortactin (33), abolished dyn-2 association with MT1-MMP–containing vesicles (Fig. S4*A*). Reciprocally, expression of a DsRed–cortactin protein lacking the SH3 domain (cortactinΔSH3) resulted in a diffuse cytosolic distribution of GFP–dyn-2 (Fig. S4*B* and quantification in Fig. 5*C*). These data demonstrate that dyn-2 colocalizes with cortactin on MT1-MMP–containing endosomes and indicate a cortactin-dependent, possibly transient association of dyn-2 with these endosomes.

The observation that loss of aPKCζ/ι activity triggered accumulation of Rab7– and MT1-MMP–positive membrane tubules (Fig. S3 *E* and *F*) prompted us to investigate whether accumulation of cortactin on MT1-MMP–containing endosomes in aPKCζ/ι-depleted cells affected dyn-2 recruitment and consequently tubule fission. To do so, we silenced aPKCζ/ι in MDA-MB-231 cells and observed a reduction of GFP–Dyn-2 recruitment associated with DsRed–cortactin patches along with increased endosomal cortactin accumulation (Fig. 4*E* and Fig. S4*C*, internal plane). Analysis of the intensity ratio of the fluorescence signals from GFP–dyn-2 and DsRed–cortactin in endosomal patches showed that the intensity ratio in aPKCζ/ι-depleted cells was reduced by 60% compared with the control—siLuc-treated—cells (Fig. 4*F*). In contrast, aPKCζ/ι knockdown did not affect the association of Dyn-2 with clathrin-coated pits at the plasma membrane (Fig. S4*C*, ventral plane). Thus, we conclude that accumulation of cortactin in the absence of aPKCζ/ι function interferes specifically with Dyn-2 recruitment on MT1-MMP–containing late endosomes. In addition, in agreement with previous findings (34), silencing of dyn-2 in MDA-MB-231 cells correlated with a substantial loss of their ability to degrade the matrix similar to the effect of cortactin knockdown (Fig. 4*G*). Accumulation of MT1-MMP–positive vesicles and tubules connected to and extending from MT1-MMP–containing endosomes was visible in Dyn-2–depleted cells (Fig. S4 *D* and *E* and Movie S3). Collectively, these data indicate that dyn-2 acts downstream of cortactin and that aPKCζ/ι is required for the formation and function of cortactin–dyn-2 assemblies on multivesicular bodies/late endosomes, suggesting a mechanism involved in the formation and fission of tubulovesicular carriers from these endosomes.

aPKCζ/ι-Dependent Phosphorylation of Cortactin Controls Its Association with dyn-2. We then addressed how aPKCζ/ι controls cortactin and dyn-2 association on MT1-MMP–containing endosomes. We tested whether cortactin was a direct substrate for aPKCζ/ι by incubating purified GST-tagged human cortactin in the presence of recombinant human aPKCι. Phosphorylation was detected with antibodies raised against cortactin phospho-Ser298, which was recently identified as a phosphorylation site for aPKCζ/ι-related PKD (35, 36). In higher metazoans, mRNA splicing generates cortactin variants with four, five, or six conserved tandem actin-binding repeats in which repeats 5 and 6 are the most conserved (37). The cortactin variant used for this study contains five tandem repeats; Ser261 in repeat 5 is highly conserved and equivalent to Ser298 in repeat 6. Recombinant aPKCι induced phosphorylation of recombinant human cortactin (Fig. 5*A*). In addition, coexpression of the five repeat-containing cortactin variant (33) with aPKCι in MDA-MB-231 cells similarly resulted in phosphorylation of cortactin (Fig. 5*B*). Thus, our data suggest that Ser261 is directly phosphorylated by aPKCι.

Next, we investigated the consequences of substitution of serine 261 to alanine (nonphosphorylable mutation) or to aspartate (phosphomimetic mutation) on gelatin degradation.

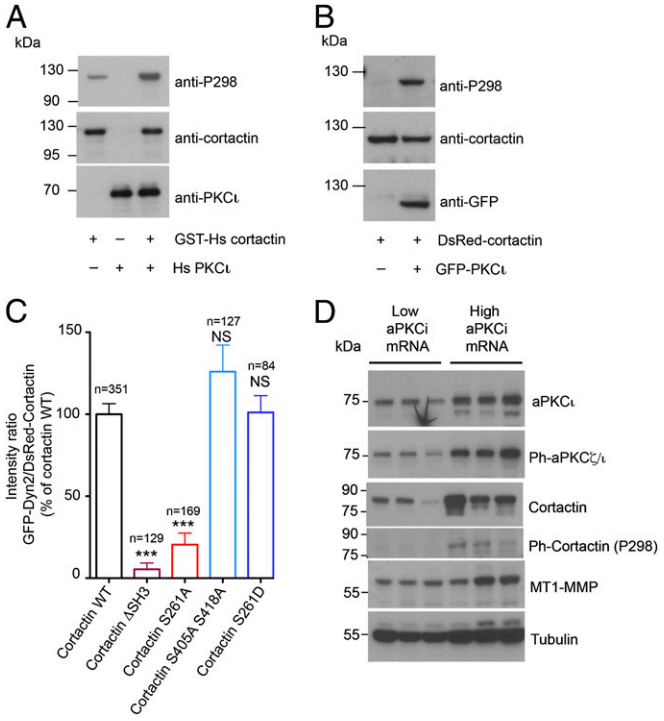

Fig. 5. Phosphorylation of cortactin by aPKCι controls dyn-2 association with cytoplasmic cortactin-positive puncta. (*A*) Purified GST-tagged human cortactin (2 μg) was incubated in the presence (0.5 μg) or absence of recombinant human aPKCι for 20 min at 37 °C. Cortactin phosphorylation was analyzed by immunoblotting with antibodies against cortactin pSer298 phosphopeptide (anti-P298). (*B*) Lysates of MDA-MB-231 cells expressing DsRed–cortactin alone or together with GFP–aPKCι were analyzed by immunoblotting with antibodies against pSer298 (anti-P298), total cortactin, or GFP. (*C*) Quantification of dyn-2 on cortactin patches from confocal dual-color spinning-disk images of MDA-MD-231 cells overexpressing GFP–dyn-2 together with DsRed-tagged wild-type cortactin or variants as indicated. The ratios of the signal intensities from dyn-2 and cortactin were measured from *n* endosome patches. ***$P < 0.001$; NS, not significant. (*D*) Whole-cell extracts from breast tumors underexpressing (low) or overexpressing (high) aPKCι mRNA were analyzed by immunoblotting with the indicated antibodies. Tubulin was used as a control for equal loading.

Overexpression of cortactin S261A in BT-549 cells led to an ∼50% reduction in matrix degradation whereas cortactin S261D had the opposite stimulatory effect (Fig. S4*F*). In addition, similar to the loss of aPKCζ/ι (Fig. 4 *E* and *F*), expression of cortactin-S261A caused drastic and specific depletion of dyn-2 from endosomal patches (Fig. 5*C* and Fig. S4*G*). By contrast, mutation of the extracellular signal-regulated serine/threonine kinase (ERK1/2) phosphorylation sites S405 and S418 of cortactin into alanine did not affect dyn-2 association with endosomes (Fig. 5*C*). Overexpression of the phosphomimetic cortactin S261D variant did not affect significantly dyn-2 recruitment on MT1-MMP–containing endosomes (Fig. 5*C*), suggesting that aPKCζ/ι-mediated phosphorylation of cortactin may also affect the dynamics of dyn-2 association to MT1-MMP–positive late endosomes. Finally, we observed that, in breast tumors, increased total phosphorylated aPKCι correlated with high cortactin expression and phosphorylation at the aPKCι-specific site in the actin-binding repeats (Fig. 5*D*). Together, our data indicate that aPKCι-mediated phosphorylation of cortactin regulates endosomal accumulation of cortactin and its association with dyn-2 to control MT1-MMP–positive endosome dynamics during the invasive program of breast-tumor cells.

Discussion

In this study, we report an unprecedented function for aPKCζ/ι in the invasion of breast-tumor cells. Our data show that aPKCζ/ι silencing in two breast-adenocarcinoma cell lines representative of triple-negative breast cancers inhibits MT1-MMP–dependent matrix degradation and tumor-cell invasion, while having no effect on MT1-MMP expression. Instead, aPKCζ/ι controls the trafficking and plasma-membrane targeting of MT1-MMP to invadopodia. In MDA-MB-231 and BT-549 cells, aPKCζ/ι associates partially with cortactin and its binding partners, F-actin and dyn-2, in patches on late endosomes that contain an intracellular reservoir of the transmembrane metalloproteinase MT1-MMP. aPKCζ/ι phosphorylates cortactin directly, and depletion of the kinase interferes with cortactin-dependent recruitment of the membrane scission protein dyn-2, correlating with tubulation of endosomal membranes and impaired trafficking and exocytosis of MT1-MMP to the cell surface. Thus, we conclude that aPKCζ/ι promotes the formation of transport vesicles carrying MT1-MMP (and possibly other proteins involved in invasion such as integrins) (38) from its intracellular reservoir in late endosomes to the cell surface, where it contributes to preparing the extracellular matrix for the invasion of the tumor cells. Consistent with this mechanism, our analysis of breast-tumor biopsies shows overexpression of both aPKCι and MT1-MMP in the most aggressive hormone receptor-negative HER2$^+$ and triple-negative subtypes. These proteins are found at cell–cell contacts and in intracellular vesicles in carcinoma cells, contrasting with their distinct locations on the apical and lateral plasma membranes, respectively, in healthy breast epithelial cells. The positive correlation between MT1-MMP and aPKCι mRNA expression in clinical samples was associated with poor prognosis, underscoring the functional importance of the kinase in progress of the disease.

The direct phosphorylation of cortactin residue S261 by aPKCι, as well as the association of aPKCι with cortactin-enriched domains on MT1-MMP–containing intracellular compartments, suggests that aPKCι phosphorylates cortactin on MT1-MMP–containing late endosomes. The accumulation of hypophosphorylated cortactin in aPKCζ/ι-depleted cells or in the Ser261Ala mutant inhibited association of dyn-2 with cortactin-positive patches on MT1-MMP–containing endosomes, and it decreased matrix degradation. Based on the known function of dyn-2 in membrane scission on various compartments, including late endosomes (39), impaired dyn-2 recruitment onto MT1-MMP–positive late endosomes is probably responsible for the endosomal membrane tubulation we see, with adverse consequences for MT1-MMP delivery to the surface. Thus, our data reveal a role for aPKCζ/ι on late endocytic compartments and a previously unidentified mechanism of late endosome membrane remodeling based on cortactin phosphorylation by aPKC to control dyn-2 recruitment. Phosphorylation of S405 and S418 of cortactin by ERK1/2 also stimulates invadopodia formation and matrix degradation. In addition, phosphorylation of cortactin by ERK is involved in a recycling mechanism of internalized ECM components from late endosomes/lysosomes to promote cell motility (32). However, our data indicate that ERK phosphorylation sites do not contribute to dyn-2 recruitment to cortactin-positive patches, thus suggesting different mechanisms of action for aPKCζ/ι and ERK-dependent phosphorylation sites for cortactin function during tumor-cell invasion.

Recent studies have documented an essential role for actin cytoskeleton dynamics in endosome function (30, 31, 40). The mechanism emerging from these studies indicates that actin–Arp2/3 assemblies organize early endosomal membranes into functional subdomains and contribute to cargo sorting and generation of transport intermediates. Our observation that dynamic cortactin–Arp2/3–actin subdomains of MT1-MMP–containing multivesicular

bodies coincide with sites of emergence and scission of tubulovesicular MT1-MMP carriers suggests a similar key role for actin in generating transport intermediates from multivesicular bodies/late endosomes. These mechanistic insights from cells in culture are consistent with our analysis of breast-tumor samples showing up-regulation of both aPKCι and MT1-MMP associated with hormone receptor-negative aggressive breast tumors and with poor prognosis; patients whose tumors overexpressed both aPKCι and MT1-MMP had a significantly higher risk of metastasis. When taken together with the known implication of cortactin in cancer (41, 42) and the reported up-regulation of dyn-2 expression in human metastatic tumors (43), our findings identify a key role for aPKCι, cortactin, dyn-2, and MT1-MMP in aggressive epithelial breast carcinomas and emphasize the role of polarity defects and endosomal transport in breast carcinogenesis, opening new avenues for innovative therapeutic strategies in aggressive forms of breast cancers.

The redistribution of aPKCι and MT1-MMP from the apical and lateral surfaces of epithelial cells, respectively, in normal mammary ducts to cell–cell contacts and vesicles—probably endosomes—in carcinoma cells correlates with the loss of epithelial-cell polarity observed in breast tumors. This redistribution seems particularly relevant in the context of tumor progression (see also ref. 44). Apical–basal polarity requires the activity of several proteins, including the apically located PAR complex, which contains aPKCζ/ι as well as CDC42, Par3, and Par6 (18). Moreover, components of the PAR complex regulate vesicle transport in the endocytic pathway and play a critical role in the uptake and recycling of components required for epithelial integrity (45, 46). Thus, our data suggest that a mechanism of endocytic recycling of specific cargoes based on aPKCζ/ι/cortactin/dyn-2 may operate in normal epithelial cells and may be required for maintenance of apicobasolateral polarity. Like aPKCι, Par6 is up-regulated in breast tumors (47) whereas loss of Par3 promotes breast-cancer metastasis (48, 49). Collectively, these data suggest that deregulation of PAR complex components in breast carcinomas contributes to tumor progression via deregulation of cell polarity and that one major consequence of aPKCζ/ι overexpression and mislocalization in tumors is the recycling and exocytosis of MT1-MMP, promoting metastasis of carcinoma cells in most aggressive breast tumors.

Experimental Procedures

Antibodies and Plasmid Constructs. For antibodies and plasmid constructs, see *SI Experimental Procedures*.

Cell Culture, Transfection, Stable Cell Lines, and Knockdown. For cell culture, transfection, stable cell lines, and knockdown, see *SI Experimental Procedures*.

Fluorescent Gelatin Degradation Assay and Invasion Assays. Assays of fluorescent gelatin degradation were performed and quantified as previously described (15). About 250–300 cells from at least three independent experiments were analyzed for each condition. Assays to measure cell invasion into Matrigel and to measure the invasion of cells from multicellular spheroids into native type I collagen assays were performed as described previously (13, 50). The latter assays were quantified by estimating the diameter of spheroids at T0 and T2 as described (50).

Indirect Immunofluorescence Microscopy, 3D Deconvolution, and Image Analysis. MDA-MB-231 cells were cultured on gelatin-coated coverslips and processed for immunofluorescence microscopy as previously described (13). Image acquisition and analysis are described in *SI Experimental Procedures*.

Live-Cell Imaging and Analysis of MT1-MMP–Containing Endosome Movement. For live-cell imaging and analysis of MT1-MMP–containing endosome movement, see *SI Experimental Procedures*.

Total Interference Reflection Fluorescence Microscopy. Cells expressing MT1-MMP–mCherry and depleted of the proteins of interest (cortactin, aPKCζ/ι, dyn-2) by means of siRNAs were plated on cross-linked gelatin-coated glass-bottom dishes (MatTek) for 2 h before imaging. TIRFM imaging was performed on a custom setup as described previously with a penetration depth of 150–300 nm (51). MT1-MMP–mCherry at the cell surface was quantified by using integrated intensity measurement in Metamorph software.

Structured Illumination Microscopy. For structured illumination microscopy, see *SI Experimental Procedures*.

Electron Microscopy. For electron microscopy, see *SI Experimental Procedures*.

Human Samples and Clinical and Tissue Microarray Data. Our series of cases was composed of 68 cases of invasive ductal carcinoma representative of each molecular subtype of breast cancer: i.e., luminal A, luminal B, ER^- PR^- $HER2^+$, and ER^- PR^- $HER2^-$ (triple-negative). Clinicopathological parameters of breast-cancer cases examined are described in Dataset S1. Breast molecular subtypes were defined as follows: luminal A+B according to ref. 52 [luminal A, estrogen receptor (ER) ≥ 10%, progesterone receptor (PR) ≥ 20%, Ki67 < 14%; luminal B, ER ≥ 10%, PR < 20%, Ki67 ≥ 14%]; ER^- PR^- $HER2^+$, ER < 10%, PR < 10%, HER2 2+ amplified or 3+ according to ref. 53; ER^- PR^- $HER2^-$ (triple-negative), ER < 10%, PR < 10%, HER2 0/1+ or 2+ nonamplified according to American Society of Clinical Oncology (ASCO) guidelines (53). MT1-MMP and aPKCι expression and association with clinicopathological features of breast cancer were assessed by IHC analysis of a breast-cancer tissue microarray (TMA) of invasive ductal carcinoma. TMA consisted of replicate tumor cores (1-mm diameter) selected from whole-tumor tissue section in the most representative tumor areas (high tumor-cell density) of each tumor sample and a matched tissue core from adjacent nontumoral breast epithelium (referred to as normal breast tissue). Immunohistocytochemistry staining was performed according to previously published protocols (54).

Analyses were performed in accordance with the French Bioethics Law 2004–800 and the French National Institute of Cancer (INCa) Ethics Charter and after approval by the Institut Curie review board and ethics committee (Comité de Pilotage du Groupe Sein), which waived the need for written informed consent from the participants. Women were informed of the research use of their tissues and did not declare any opposition for such research. Data were analyzed anonymously.

RNA Extraction and Real-Time PCR Analysis. For RNA extraction and real-time PCR analysis, see *SI Experimental Procedures*.

Statistical Analyses. Relationships between mRNA levels of various target genes and comparison of target-gene mRNA levels with clinical parameters were estimated by using the χ^2 test (for links between two qualitative parameters) and the Spearman rank correlation test (for links between two quantitative parameters). Differences between the two populations were judged significant at confidence levels greater than 95% ($P < 0.05$). Metastasis-free survival (MFS) was determined as the interval between diagnosis and detection of the first metastasis. Survival distributions were estimated by the Kaplan–Meier method, and the significance of differences between survival rates was ascertained using a log-rank test. Relationships between protein expression and distribution in tumors vs. normal adjacent tissues were estimated using the Kruskal–Wallis test (for links between qualitative and quantitative parameters). Other statistical analyses were performed using the ANOVA or Student *t* test (link between one qualitative parameter and one quantitative parameter) in Prism software.

ACKNOWLEDGMENTS. We thank Drs. M. Arpin, T. Galli, and M. A. McNiven for providing reagents. We acknowledge the Breast Cancer Study Group of Institut Curie headed by Drs. B. Sigal-Zafrani and T. Dubois (Transfer Department, Institut Curie) and the patients for the breast-tumor samples. C.R. and P.M. were supported by a fellowship from the Fondation ARC pour la Recherche sur le Cancer (ARC). L.F. and M.N. were supported by the Incentive and Cooperative Research Programme "Breast Cancer: Cell Invasion and Motility" of Institut Curie. Funding for this work was provided by ARC Grant SL220100601356, by Agence Nationale pour la Recherche Grant ANR-08-BLAN-0111 and Institut National du Cancer Grant 2012-1-PL BIO-02-IC-1 (to P.C.), and by core funding from Institut Curie and the Centre National pour la Recherche Scientifique. We acknowledge France-BioImaging infrastructure supported by the French National Research Agency (ANR-10-INSB-04, Investments for the future).

1. Egeblad M, Werb Z (2002) New functions for the matrix metalloproteinases in cancer progression. *Nat Rev Cancer* 2(3):161–174.
2. Kessenbrock K, Plaks V, Werb Z (2010) Matrix metalloproteinases: Regulators of the tumor microenvironment. *Cell* 141(1):52–67.
3. Sato H, et al. (1994) A matrix metalloproteinase expressed on the surface of invasive tumour cells. *Nature* 370(6484):61–65.
4. Strongin AY, et al. (1995) Mechanism of cell surface activation of 72-kDa type IV collagenase: Isolation of the activated form of the membrane metalloprotease. *J Biol Chem* 270(10):5331–5338.
5. Hotary KB, et al. (2003) Membrane type I matrix metalloproteinase usurps tumor growth control imposed by the three-dimensional extracellular matrix. *Cell* 114(1): 33–45.
6. Hotary K, Li XY, Allen E, Stevens SL, Weiss SJ (2006) A cancer cell metalloprotease triad regulates the basement membrane transmigration program. *Genes Dev* 20(19): 2673–2686.
7. Wolf K, et al. (2007) Multi-step pericellular proteolysis controls the transition from individual to collective cancer cell invasion. *Nat Cell Biol* 9(8):893–904.
8. Jiang WG, et al. (2006) Expression of membrane type-1 matrix metalloproteinase, MT1-MMP in human breast cancer and its impact on invasiveness of breast cancer cells. *Int J Mol Med* 17(4):583–590.
9. Perentes JY, et al. (2011) Cancer cell-associated MT1-MMP promotes blood vessel invasion and distant metastasis in triple-negative mammary tumors. *Cancer Res* 71(13):4527–4538.
10. Artym VV, Zhang Y, Seillier-Moiseiwitsch F, Yamada KM, Mueller SC (2006) Dynamic interactions of cortactin and membrane type 1 matrix metalloproteinase at invadopodia: Defining the stages of invadopodia formation and function. *Cancer Res* 66(6):3034–3043.
11. Murphy DA, Courtneidge SA (2011) The 'ins' and 'outs' of podosomes and invadopodia: characteristics, formation and function. *Nat Rev Mol Cell Biol* 12(7): 413–426.
12. Poincloux R, Lizárraga F, Chavrier P (2009) Matrix invasion by tumour cells: A focus on MT1-MMP trafficking to invadopodia. *J Cell Sci* 122(Pt 17):3015–3024.
13. Steffen A, et al. (2008) MT1-MMP-dependent invasion is regulated by TI-VAMP/ VAMP7. *Curr Biol* 18(12):926–931.
14. Clark ES, Whigham AS, Yarbrough WG, Weaver AM (2007) Cortactin is an essential regulator of matrix metalloproteinase secretion and extracellular matrix degradation in invadopodia. *Cancer Res* 67(9):4227–4235.
15. Sakurai-Yageta M, et al. (2008) The interaction of IQGAP1 with the exocyst complex is required for tumor cell invasion downstream of Cdc42 and RhoA. *J Cell Biol* 181(6): 985–998.
16. Williams KC, Coppolino MG (2011) Phosphorylation of membrane type 1-matrix metalloproteinase (MT1-MMP) and its vesicle-associated membrane protein 7 (VAMP7)-dependent trafficking facilitate cell invasion and migration. *J Biol Chem* 286(50):43405–43416.
17. Mellor H, Parker PJ (1998) The extended protein kinase C superfamily. *Biochem J* 332(Pt 2):281–292.
18. McCaffrey LM, Macara IG (2011) Epithelial organization, cell polarity and tumorigenesis. *Trends Cell Biol* 21(12):727–735.
19. Rosse C, et al. (2009) An aPKC-exocyst complex controls paxillin phosphorylation and migration through localised JNK1 activation. *PLoS Biol* 7(11):e1000235.
20. Sun R, et al. (2005) Protein kinase C zeta is required for epidermal growth factor-induced chemotaxis of human breast cancer cells. *Cancer Res* 65(4):1433–1441.
21. Rodriguez EM, Dunham EE, Martin GS (2009) Atypical protein kinase C activity is required for extracellular matrix degradation and invasion by Src-transformed cells. *J Cell Physiol* 221(1):171–182.
22. Kojima Y, et al. (2008) The overexpression and altered localization of the atypical protein kinase C lambda/iota in breast cancer correlates with the pathologic type of these tumors. *Hum Pathol* 39(6):824–831.
23. Awadelkarim KD, et al. (2012) Quantification of PKC family genes in sporadic breast cancer by qRT-PCR: Evidence that PKCι/λ overexpression is an independent prognostic factor. *Int J Cancer* 131(12):2852–2862.
24. Regala RP, et al. (2005) Atypical protein kinase C iota is an oncogene in human non-small cell lung cancer. *Cancer Res* 65(19):8905–8911.
25. Sørlie T, et al. (2001) Gene expression patterns of breast carcinomas distinguish tumor subclasses with clinical implications. *Proc Natl Acad Sci USA* 98(19):10869–10874.
26. Neve RM, et al. (2006) A collection of breast cancer cell lines for the study of functionally distinct cancer subtypes. *Cancer Cell* 10(6):515–527.
27. Sabeh F, Shimizu-Hirota R, Weiss SJ (2009) Protease-dependent versus -independent cancer cell invasion programs: Three-dimensional amoeboid movement revisited. *J Cell Biol* 185(1):11–19.
28. Lizárraga F, et al. (2009) Diaphanous-related formins are required for invadopodia formation and invasion of breast tumor cells. *Cancer Res* 69(7):2792–2800.
29. Miesenbock G (2012) Synapto-pHluorins: Genetically encoded reporters of synaptic transmission. *Cold Spring Harb Protoc* 2012(2):213–217.
30. Derivery E, et al. (2009) The Arp2/3 activator WASH controls the fission of endosomes through a large multiprotein complex. *Dev Cell* 17(5):712–723.
31. Puthenveedu MA, et al. (2010) Sequence-dependent sorting of recycling proteins by actin-stabilized endosomal microdomains. *Cell* 143(5):761–773.
32. Sung BH, Zhu X, Kaverina I, Weaver AM (2011) Cortactin controls cell motility and lamellipodial dynamics by regulating ECM secretion. *Curr Biol* 21(17):1460–1469.
33. McNiven MA, et al. (2000) Regulated interactions between dynamin and the actin-binding protein cortactin modulate cell shape. *J Cell Biol* 151(1):187–198.
34. Baldassarre M, et al. (2003) Dynamin participates in focal extracellular matrix degradation by invasive cells. *Mol Biol Cell* 14(3):1074–1084.
35. Eiseler T, Hausser A, De Kimpe L, Van Lint J, Pfizenmaier K (2010) Protein kinase D controls actin polymerization and cell motility through phosphorylation of cortactin. *J Biol Chem* 285(24):18672–18683.
36. Rozengurt E (2011) Protein kinase D signaling: Multiple biological functions in health and disease. *Physiology (Bethesda)* 26(1):23–33.
37. van Rossum AG, Schuuring-Scholtes E, van Buuren-van Seggelen V, Kluin PM, Schuuring E (2005) Comparative genome analysis of cortactin and HS1: The significance of the F-actin binding repeat domain. *BMC Genomics* 6:15.
38. Dozynkiewicz MA, et al. (2012) Rab25 and CLIC3 collaborate to promote integrin recycling from late endosomes/lysosomes and drive cancer progression. *Dev Cell* 22(1): 131–145.
39. Schroeder B, Weller SG, Chen J, Billadeau D, McNiven MA (2010) A Dyn2-CIN85 complex mediates degradative traffic of the EGFR by regulation of late endosomal budding. *EMBO J* 29(18):3039–3053.
40. Harrington AW, et al. (2011) Recruitment of actin modifiers to TrkA endosomes governs retrograde NGF signaling and survival. *Cell* 146(3):421–434.
41. Luo ML, et al. (2006) Amplification and overexpression of CTTN (EMS1) contribute to the metastasis of esophageal squamous cell carcinoma by promoting cell migration and anoikis resistance. *Cancer Res* 66(24):11690–11699.
42. Clark ES, et al. (2009) Aggressiveness of HNSCC tumors depends on expression levels of cortactin, a gene in the 11q13 amplicon. *Oncogene* 28(3):431–444.
43. Eppinga RD, et al. (2012) Increased expression of the large GTPase dynamin 2 potentiates metastatic migration and invasion of pancreatic ductal carcinoma. *Oncogene* 31(10):1228–1241.
44. Huang L, Muthuswamy SK (2010) Polarity protein alterations in carcinoma: A focus on emerging roles for polarity regulators. *Curr Opin Genet Dev* 20(1):41–50.
45. Leibfried A, Fricke R, Morgan MJ, Bogdan S, Bellaiche Y (2008) Drosophila Cip4 and WASp define a branch of the Cdc42-Par6-aPKC pathway regulating E-cadherin endocytosis. *Curr Biol* 18(21):1639–1648.
46. Winter JF, et al. (2012) Caenorhabditis elegans screen reveals role of PAR-5 in RAB-11-recycling endosome positioning and apicobasal cell polarity. *Nat Cell Biol* 14(7): 666–676.
47. Nolan ME, et al. (2008) The polarity protein Par6 induces cell proliferation and is overexpressed in breast cancer. *Cancer Res* 68(20):8201–8209.
48. McCaffrey LM, Montalbano J, Mihai C, Macara IG (2012) Loss of the Par3 polarity protein promotes breast tumorigenesis and metastasis. *Cancer Cell* 22(5):601–614.
49. Xue B, Krishnamurthy K, Allred DC, Muthuswamy SK (2013) Loss of Par3 promotes breast cancer metastasis by compromising cell-cell cohesion. *Nat Cell Biol* 15(2): 189–200.
50. Rey M, Irondelle M, Waharte F, Lizarraga F, Chavrier P (2011) HDAC6 is required for invadopodia activity and invasion by breast tumor cells. *Eur J Cell Biol* 90(2-3): 128–135.
51. Montagnac G, et al. (2011) Decoupling of activation and effector binding underlies ARF6 priming of fast endocytic recycling. *Curr Biol* 21(7):574–579.
52. Prat A, et al. (2013) Prognostic significance of progesterone receptor-positive tumor cells within immunohistochemically defined luminal A breast cancer. *J Clin Oncol* 31(2):203–209.
53. Wolff AC, et al. (2007) American Society of Clinical Oncology/College of American Pathologists guideline recommendations for human epidermal growth factor receptor 2 testing in breast cancer. *J Clin Oncol* 25(1):118–145.
54. Vincent-Salomon A, et al. (2007) HER2 status of bone marrow micrometastasis and their corresponding primary tumours in a pilot study of 27 cases: A possible tool for anti-HER2 therapy management? *Br J Cancer* 96(4):654–659.